Published in final edited form as:
J Biomed Mater Res A. 2011 September 15; 98(4): 509–516. doi:10.1002/jbm.a.33128.

A Chemically Polymerized Electrically Conducting Composite of Polypyrrole Nanoparticles and Polyurethane for Tissue Engineering

Christopher R. Broda[1,*], **Jae Y. Lee**[2], **Sirinrath Sirivisoot**[3], **Christine E. Schmidt**[2,4], and **Benjamin S. Harrison**[3]

[1]School of Medicine, Wake Forest University, Winston-Salem, NC

[2]Department of Chemical Engineering, University of Texas at Austin, Austin, TX

[3]Wake Forest Institute for Regenerative Medicine, Wake Forest University, Winston-Salem, NC

[4]Department of Biomedical Engineering, University of Texas at Austin, Austin, TX

Abstract

A variety of cell types respond to electrical stimuli, accordingly many conducting polymers (CPs) have been used as tissue engineering (TE) scaffolds, one such CP is polypyrrole (PPy). PPy is a well studied biomaterial with potential TE applications due to its electrical conductivity and many other beneficial properties. Combining its characteristics with an elastomeric material, such as polyurethane (PU), may yield a hybrid scaffold with electrical activity and significant mechanical resilience. Pyrrole was *in situ* polymerized within a PU emulsion mixture in weight ratios of 1:100, 1:20, 1:10 and 1:5, respectively. Morphology, electrical conductivity, mechanical properties and cytocompatibility with C2C12 myoblast cells were characterized. The polymerization resulted in a composite with a principle base of PU interspersed with an electrically percolating network of PPy nanoparticles. As the mass ratio of PPy to PU increased so did electrical conductivity of the composites. In addition, as the mass ratio of PPy to PU increased, stiffness of the composite increased while maximum elongation length decreased. Ultimate tensile strength was reduced by approximately 47% across all samples with the addition of PPy to the PU base. Cytocompatibility assay data indicated no significant cytotoxic effect from the composites. Static cellular seeding of C2C12 cells and subsequent differentiation showed myotube formation on the composite materials.

Keywords

Tissue Engineering; Polyurethane; Polypyrrole; Myoblast; Electrical Conduction

Introduction

Electrically conducting polymers (CP) have long been recognized as advantageous substrates for tissue engineering (TE) scaffolds. Many cell types including neurons[1, 2], osteoblasts[3, 4], fibroblasts[5] and skeletal myoblasts[6] (SMs) respond to electrical stimuli. Because of this fact, CPs' unique properties have been applied to many biomedical applications[7]. One of the most extensively studied CPs, polypyrrole (PPy), has demonstrated characteristics essential for many biomedical applications including TE. Of particular interest, PPy has demonstrated biocompatibility[8–10] and modulation of adhesion,

*Corresponding author: Christopher R. Broda (chbroda@wfubmc.edu).

proliferation and differentiation of many cells types including endothelial cells[11], rat pheochromocytoma cells[12], and SMs[13]. Other positive attributes of PPy include the ability to entrap and controllably release biomolecules, the capacity to undergo reversible doping, and their potential ease of modification[14]. Despite these beneficial properties, PPy is generally brittle and would be inappropriate for use as a TE scaffold in many *in vivo* environments that encounter intense mechanical forces.

PPy is often used in conjunction with other biomaterials for TE applications for enhanced properties, including mechanical integrity and electrical conductivity[15, 16]. Therefore, polymer composites containing PPy can provide the mechanical property profile necessary for many TE applications while retaining the beneficial properties of PPy. Polyurethanes (PUs) have an excellent reputation as biocompatible, highly durable materials for biomedical applications including heart valves, aortic grafts, dialysis membranes, indwelling catheters, intra-aortic balloons and mammary implants[17, 18]. The high tensile strength, flexural fatigue and biocompatibility of PU have not gone unrecognized within the TE community. Others have applied PU as a scaffold in TE paradigms using a variety of cell types including smooth muscle cells[19], cardiomyocytes[20], osteoblasts[21], neurons[22], and SMs[23] demonstrating biocompatibility and enhancement of cellular processes.

Combining the electrical properties of PPy and the mechanical resilience of PU in a composite biomaterial may enable electrical cellular modulation in a mechanically stressful environment. The hybrid material may facilitate both mechanical and electrical communication of cells within the neotissue itself, and may provide enhanced integration of the tissue engineered construct and host. Perhaps not surprisingly, others have investigated PPy enhanced elastomers in other biomedical applications[24]. Although there have been several attempts to synthesize PPy-PU composites [25, 26], the authors know of no relevant studies that characterize such composites for use in TE with SMs. The hybrid material was polymerized using an *in situ* polymerization emulsion technique. Electrical conductance, morphological and mechanical characterization were assessed because these physical properties are relevant with regard to TE. Additionally, cytocompatibility and cellular differentiation assays (myotube formation) with SMs were assessed on the PPy nanoparticle and PU composites in this study. The results of this preliminary work will be utilized in futures studies investigating the potential of a PPy nanoparticle and PU composite as an electromechanical coupler for SMs in a cardiac tissue engineering paradigm.

Materials and Methods

Materials

Carbothane PC-3585A (PU) was generously donated by Lubrizol. All chemicals, cell culture supplements, and disposable tissue culture supplies were purchased from Aldrich, Sigma, and BD, respectively, and used as received unless otherwise noted.

PPy-PU Composite synthesis

The *in situ* chemical polymerization of pyrrole (Py) in a mixture with PU to create a composite material was based on a modification of a protocol described by Wang, Z *et al*[27]. Py monomer (Aldrich) was purified with activated basic alumina (Aldrich) before use. 10 % w/v PU dissolved in $CHCl_3$ (Fisher) was prepared at least 24 hours prior to use. An emulsion mixture of purified Py in the appropriate weight ratio and PU in $CHCl_3$ was created by adding 1% w/v sodium lauryl sulfate (SDS) (Bio-Rad Laboratories) and vigorously stirring for 0.5 hour. For example, 0.25 grams of SDS was added to a solution of 2.5 grams of PU dissolved in 25 mL of $CHCl_3$. 0.3 M $FeCl_3$ (Aldrich) was added dropwise via syringe and 21 G needle (BD) to the vigorously stirring emulsion solution at a molar

ratio stoichiometric excess of 2.3 moles $FeCl_3$ to 1 mole Py. Weight ratios reported in this study are based on the preload of Py and assume complete polymerization. After 3 hours, the reaction was quenched with anhydrous ethanol followed by washing in anhydrous ethanol (Biopharm). Then the composite, being still malleable, was pressed to a 1 mm thickness and allowed to set at room temperature under a nominal vacuum. Finally, the composite was dried and stored in a vacuum chamber for at least 48 hours to ensure solvent vaporization.

A 10% w/v PU in $CHCl_3$ solution was used to solvent cast pure PU films as controls in a glass petri dish. These films were allowed to set at room temperature under a nominal vacuum and stored under vacuum for at least 48 hours to ensure solvent vaporization.

Physiochemical characterization

Microscopic morphological characterization was performed using scanning electron microscopy (SEM) (Carl Zeiss SMT, LEO 1530). Composites were flash frozen with liquid nitrogen and broken to image the inner content of the material. Samples that were not sufficiently conductive were sputter coated with 5 nm of platinum/palladium using a sputter coater (Cressington Scientific Instruments, Model 208HR). Particle size was analyzed from the SEM images of the composites using ImageJ software (NIH, version 1.43). The individual diameters of randomly selected nanoparticles particles (n=75) were measured from the SEM images acquired from non-sputter coated composite cross-sections. This was performed for two samples from each different weight ratio composite utilizing the measurement scale provided by the SEM image capture software.

To study electrical properties of the PPy-PU composites, resistivities (n=3 different points per sample) were measured by four-point probe method (CH Instruments) under ambient conditions. Briefly, the four-point probe method allows for the measure of electrical impedance of a material via the application of a current and measurement of voltage change and is more accurate than traditional two terminal sensing modalities. Conductivity was calculated using a derivation of Ohm's law to factor in the geometry of the test materials[28, 29]. The equations used are as follows:

$$V=IR \tag{1}$$

$$\rho=\frac{\pi}{\ln(2)}t\frac{V}{I} \tag{2}$$

$$\sigma=\rho^{-1} \tag{3}$$

where V is voltage, I is current, R is resistance, ρ is the bulk resistivity, t is thickness, σ is the conductivity of the material. Equation (1) is Ohm's law and is required to derive equation (2) the answer of which is then plugged into equation (3).

Mechanical properties of composites were measured using an Instron 5544 (Instron). Experimental materials were formed using a 10 mm × 20 mm dog-bone die (n=6). Each specimen was loaded to failure at an extension rate of 10.0 mm/min. Blue Hill software was used for data acquisition and processing. Young's modulus was calculated from the most linear slope of the stress/strain relationship between each sample.

In vitro cytocompatibility and composite-cell interactions

C2C12 murine myoblasts (ATCC) were expanded and maintained in Dulbecco's modified Eagle's medium (high glucose DMEM, Sigma) containing 10% fetal bovine serum (FBS)

(Hyclone) and 1% penicillin/streptomycin (P/S) (Sigma). Experimental materials were sterilized by immersion in 70% ethanol for 3 hours and 30 minutes UV exposure to each side. C2C12 myoblasts (p=5) were seeded at a cell density of 10^5 cells per well in a 24 well tissue culture plate (BD) and incubated (5% CO_2, humidified air). After 24 hours in culture, the media was changed and the experimental materials (n=3) were added. Following 48 hours incubation, the experimental materials were removed and cytotoxicity was assessed using an MTS assay kit (Promega). A plate reader was used to measure the conversion of the tetrazolium salt to its colormetric indicator at a wavelength of 490 nm.

C2C12 myoblasts (p=34) were seeded at 2.5×10^5, 5.0×10^5, 1.0×10^6 cells per cm^2 on PU and composite materials and cultured for 24 hours. Experimental groups were fixed in 2.5% glutaraldehyde (Sigma) for 2 hours and dehydrated in a series of graded ethanol solutions. Samples were subsequently prepared by critical point drying (Electron Microscopy Sciences, EMS850X), sputter coated with gold under vacuum with an applied current of 15 mA for 2 minutes (Anatech, Hummer 6.2), and then imaged via SEM (Hitachi, S-2600N).

For myotube differentiation of C2C12 myoblasts, PU and PPy-PU composites were seeded with C2C12 cells (p=10) at a density of 5.0×10^5 cells/cm^2 then cultured in complete media containing DMEM + 20% FBS + 1% chick embryo extract (Sera Laboratories International Ltd.) + 2% horse serum (Hyclone) + 1% P/S for 6 days (5% CO_2, humidified air). To assess differentiation, myotubes were stained with anti-myosin heavy chain (MHC) MF20 (1:20, Developmental Studies Hybridoma Bank) antibody and nuclear contents were marked with DAPI using standard immunocytochemical techniques[30]. The secondary antibody was fluorescein-conjugated horse anti-mouse (1:200, Vector). Samples were visualized using a Zeiss AxioImager M1 fluorescence microscope.

Statistical Analysis

Results are expressed as mean ± standard deviation. Statistical analyses were performed using analysis of variance (ANOVA) with a Bonferroni *post hoc* test when comparing multiple means. Probability values (p) for significance were calculated; $p < 0.05$ was considered significant.

Results

PPy-PU composite synthesis

The oxidative chemical polymerization of Py with dropwise addition of $FeCl_3$ led to black precipitate in all composites, inferring PPy formation. However, it was impossible to delineate between the PPy and PU phases with gross observation.

Physicochemical characterization

Morphologies of the composites were analyzed using scanning electron microscopy (Figure 2). Overall, the trans-section of all PPy-PU samples exhibited well-dispersed PPy nanoparticles in PU; however, some particle aggregates were found in the composites with lower PPy contents (e.g., 1:100, 1:20). We also analyzed sizes of the PPy nanoparticles in the different composites. The 1:5 of PPy:PU sample contained nanoparticles with an average diameter of 238 (±69) nm, 1:10 of PPy:PU sample's particles had an average diameter of 197 (±68) nm, 1:20 of PPy:PU sample's particles had an average diameter of 185 (±67) nm and the 1:100 of PPy:PU sample's particles had an average diameter of 166 (±80) nm. Although 1:10 compared to 1:20 and 1:20 compared to 1:100 did not statistically differ, this trend of decreasing nanoparticle size in relation to less PPy content is probably due to the emulsifier to Py ratio during polymerization, as the amount of SDS did not change.

Electrical conductivity of the PPy nanoparticles and PU composites was analyzed using a four-point probe. Commonly reported conductivities of PPy prepared by chemical oxidative polymerization with $FeCl_3$ range from 0.07 to 5 S/cm[31]. As seen in Table 1, the 1:5 of PPy:PU composite had the highest conductivity [2.3×10^{-6} ($\pm3.0\times10^{-7}$) S/cm] while the 1:100 of PPy:PU composite was the least conductive composite [1.0×10^{-10} ($\pm8.0\times10^{-11}$) S/cm]. The 1:5 of PPy:PU sample's conductivity statistically differed from all other groups. The conductivity of PU, a known insulator, was not measurable using our conventional four-point probe instrument, as expected.

The addition of a PPy phase to the PU caused an alteration in mechanical properties Ultimate tensile strength (Figure 3) was decreased, on average, by about 47% with the addition of any weight ratio of PPy. None of the tensile strength values of the PPy-PU composites significantly differed except when compared to PU. Breaking elongation (Figure 4) and Young's modulus (Figure 5) were both altered in a PPy mass content dependent fashion. The lowest weight ratio compound, 1:100 of PPy:PU, demonstrated a 559 (± 70.2) % breaking length and 9.05 (± 1.32) MPa Young's modulus. The greatest weight percent composite, 1:5 of PPy:PU, demonstrated a 313 (± 82.8) % breaking length and 24.4 (± 3.73) MPa Young's modulus showing a correlation of reduction in the total elongation length and an increase in material stiffness as the PPy:PU mass ratio increased. The only samples that did not statistically differ were 1:5 compared to 1:10 and 1:10 compared to 1:20 of PPy:PU when analyzing breaking elongation. Additionally, 1:100 of PPy:PU compared to pure PU Young's moduli did not statistically differ.

Cytocompatibility

In vitro culture assays showed no statistical differences between any experimental group indicating cytocompatibility of the composites (Figure 6).

C2C12 cells were seeded onto the PPy-PU composites for 24 hours to explore cell-material interactions. All the composites of PPy nanoparticles and PU supported the cell adhesion and growth (Figure 7). Interestingly, cells cultured on PU tended to aggregate rather than spread over the surface. Also, at the lowest ratio of PPy (1:100 of PPy:PU), cells did not appear to interact well with surfaces compared to those of composites consisting higher PPy weight ratios.

The ability of the PPy-Pu composites to support SM proliferation and accommodate myotube formation was an important goal of this study. Figure 8 shows myotube formation in every composite formulation with minimal to no myotube development in the PU sample. Qualitatively, a higher density of myotube formation, evidenced by increased MHC staining, was observed on the 1:5 and 1:10 of PPy:PU samples than in the 1:20 and 1:100 of PPy:PU samples.

Discussion

We aimed to form a hybrid composite material for TE by combining PPy and PU to create an electrically conducting polymer. We selected PU polymers as the embedding matrix because they are particularly enticing elastomers for use in TE due to their mechanical properties[32]. The isocyanate segments of these polymers are essential to their flexibility and can be polymerized with other chemical moieties for material properties modulation. Specifically, aliphatic polycarbonate diol PU was chosen for this study because of its more oxidatively stable soft segment and established record of high performance in cardiac applications[33].

We employed different approaches to obtain composites of PPy nanoparticles and PU. In addition to *in situ* polymerization of PPy in PU (Figure 1), dispersion of pre-prepared PPy nanoparticles in a PU matrix was attempted by mechanical agitation and sonication; however, these methods were inadequate to separate PPy aggregates. These resultant PPy-PU composites demonstrated conductive heterogeneity throughout all loading mass percents of PPy (data not shown). Although PPy-PU composites have previously been synthesized[25, 34, 35], the chemical polymerization technique employed in the presented work is especially versatile, reproducible and promotes an embedded matrix of PPy doped with chloride (Cl) throughout the entire PU base.

Despite a primary composition of the insulative PU matrix, the emulsion mixture polymerization resulted in an electrically integrated network of PPy dispersed within the composite materials. The data indicated a trend of increasing conductivity as the mass fraction of PPy increased. The correlation of PPy concentration to conductivity of the PPy-PU composite allows for customization to obtain a composite with a desired electrical conductivity; however, determining a specific goal conductivity is not within the scope of this study. Likely, composite conductivities will be influenced by the organ targeted for tissue replacement/regeneration. Unfortunately, literature describing dynamic cell culture with electrical stimulation of conducting composite TE materials elaborating specific resistivities/conductivities and cellular modulation is somewhat sparce. However, for example, when PPy-coated scaffolds with resistivities similar to the composites produced were cultured with PC12 neuronal cells and stimulated with potentials of 10 and 100 mV/cm, cellular responses were observed[15].

Notwithstanding a comparatively low PPy to PU mass faction, the conductivity and PPy loading trend reported in this study (Table 1) is similar to other PPy with ionic dopant and PU composites[35]. Specifically, PPy and ionic dopant and PU composites with mass weight percents between 25% and 75%, calculated by mass PPy-ionic dopant complex / mass of 'neat' PU × 100%, have reported conductivities between 10^{-5} and 10^{-7} siemens, similar to the present work's mass ration of 1:5 (or in other terms 20% PPy-Cl mass / pure PU mass × 100%) with a mean conductivity value of 2.3×10^{-6} siemens. Like other work, generally as the PPy mass ratio increases, so does conductivity. As aforementioned, no specific conductivity goals were determined but, in addition to simply increasing the PPy load in the composites, many other factors may be modified in the polymerization protocol to best achieve a desired conductivity. For example, factors such as modulation of the oxidant concentration, reaction time, temperature of the reaction, washing, storage conditions, etc have been reported to affect resultant PPy with ionic dopant and PU composites' conductivity[35]. However, many investigators have devised ways to increase the conductivity of chemically polymerized PPy, therefore; multiple avenues may exist for increasing the conductivity of the composites. Future studies will more thoroughly address this issue.

PPy content also affects the mechanical properties of the PPy-PU composite (Figures 3, 4 and 5); these changes are probably due to multiple factors. The decrease in Young's modulus and breaking elongation can be accounted for by the general composite theory that the resultant material shares characteristics of both materials. In the present study, the PPy-PU composites bear mechanical properties of relatively brittle PPy and elastic PU, which are dependant on their ratios. Additionally, the nearly uniform decrease in tensile strength seen in all composite samples may be attributed to the biphasic nature of the dual component materials. Likely, the mechanical integrity of the PU base polymer was compromised by the relative paucity of chemical bonding between the PPy nanoparticles and PU. The relative brittleness and lack of chemical bonding likely created a structural discontinuity within the PU base polymer resulting in a decrease in a tensile strength. Still, the composites possess mechanical properties characteristic of the PU used in synthesis. Even at the highest weight

ratio of PPy, the composite retains mechanical properties similar to other materials used for TE[36].

Cytocompatibility is an important prerequisite for any potential TE scaffold. In addition to results shown (Figure 6), we also cultured human dermal fibroblasts for a similar cytocompatibility test and found no cytotoxicity of the composites (data not shown). These results may be due to the intrinsic biocompatible nature of the two primary constituents of the composites, PPy and PU. The PU (Carbothane) used in this study was medical grade, has proven cytocompatibility and is intended for use in cardiovascular applications. The cytocompatibility of PPy was previously discussed[7, 37]. Possible residuals of the reactants, such as oxidizing agent (Fe^{2+}/Fe^{3+}), unpolymerized Py monomers, and emulsifier were the major concerns for toxicity; however, if present at all, the data indicate no obvious deleterious effects of these potential residuals.

C2C12 cells and biomaterials interactions were more morphologically diverse in the composite samples (Figure 7). In this study, more cells were found on the surfaces of the PPy-PU composites compared to the smooth PU substrate. The surface roughness of the composites likely contributed to increased cellular adhesion of the SMs to the materials because nanometer surface roughness is known to promote cellular surface adhesion[38]. Nano-scale roughness of the PPy-PU composites was visualized on the topographically diverse SEM images in Figure 2. Because PU has consistently demonstrated cytocompatibility, the relative dearth of cells seen in the ×250 image of the PU group in Figure 7 (group E, image 1) is likely a result of poor cell-to-substrate attachment which may have lead to cell dislodgement. In general, little cellular material could be found on these PU substrates. Though no formal assays quantitating cell adhesion were performed, Figure 7 demonstrates morphologically diverse cell-material interactions in all composite samples. Thus, SM adhesion on the composites appears to be highly influenced be surface roughness and surface energy. Future studies will attempt to quantify the relationship of PPy to PU mass fraction and cell adhesion.

Additionally, the composites appeared to better support C2C12 proliferation and differentiation compared to pure PU (Figure 8). Myotube formation from SMs, a final step in myogenesis, requires abundant cellular communication as SMs must assemble into a complex organization of sarcomeres and myofibrils[39]. Thus, these collective *in vitro* data could be indirect evidence that the electrically conducting PPy nanoparticles and PU composite allow for enhanced cell to cell interactions via electrical integration provided by the substrate. Future studies will attempt to quantify these results and determine if they are due to differences in conductivity, surface energy, or a combination of both. Elucidation of electrical conductivity and cellular modulation with and without external electrical stimuli will be an additional goal of these prospective studies.

This study is a preliminary report on the physical and biological characteristics of a material that can be applied to TE including but not limited to cardiovascular, neural and orthopaedic applications. The significance of this project was the synthesis of a biocompatible electrically conducting material of PPy nanoparticles and PU with mechanical properties germane to various TE applications. Other investigators have created electroactive materials for TE applications[7, 40], none have described PPy nanoparticle and PU composite mechanical and electrical properties in the context of cellular compatibility. Because this is a proof-of-concept study, further studies are needed to investigate cellular interactions in dynamic culture including electrical stimulation with PPy-PU composites.

Conclusion

In this study, we showed that the electrically conducting PPy nanoparticle and PU composites were fabricated via an *in situ* chemical polymerization of Py monomers in a PU emulsion mixture with the drop-wise addition of an oxidant. The resultant PPy nanoparticles and PU composites demonstrated elastomeric properties, conductivity, and proved to be cytocompatible with C2C12 cells. The creation of an electrically percolating network within the elastomer allows for further exploration with PPy nanoparticle and PU composite materials as a potential electromechanical coupler of cells in tissue engineering paradigms.

Supplementary Material

Refer to Web version on PubMed Central for supplementary material.

Acknowledgments

We would like to thank Mitchell Ladd for his editorial assistance. This project was supported by the NIH grant R01EB003416 and by the Wake Forest Institute for Regenerative Medicine's Medical Student Research Scholarship.

Reference List

1. Jaffe L, Poo M. Neurites grow faster towards the cathode than the anode in a steady field. Journal of Experimental Zoology. 1979; 209:115–128. [PubMed: 490126]
2. Kerns J, Pavkovic I, Fakhouri A, Wickersham K, Freeman J. An experimental implant for applying a DC electrical field to peripheral nerve. Journal of Neuroscience Methods. 1987; 19:217–223. [PubMed: 3494891]
3. Bassett C, Mitchell S, Gaston S. Treatment of ununited tibial diaphyseal fractures with pulsing electromagnetic fields. Journal of Bone and Joint Surgery American Volume. 1981; 63:511–523.
4. Bassett C, Pawluk R, Becker R. Effects of electric currents on bone in vivo. Nature. 1964; 204:652–654. [PubMed: 14236279]
5. Giaever I, Keese C. Monitoring fibroblast behavior in tissue culture with an applied electric field. Proceedings of the National Academy of Sciences of the United States of America. 1984; 81:3761–3764. [PubMed: 6587391]
6. Pedrotty DM, Koh J, Davis BH, Taylor DA, Wolf P, Niklason LE. Engineering skeletal myoblasts: Roles of three-dimensional culture and electrical stimulation. American Journal of Physiology, Heart and Circulatory Physiology. 2005; 288:1620–1626.
7. Guimard NK, Gomez N, Schmidt CE. Conducting polymers in biomedical engineering. Progress in Polymer Science. 2007; 32:876–921.
8. Williams R, Doherty P. A preliminary assessment of poly(pyrrole) in nerve guide studies. Journal of Materials Science: Materials in Medicine. 1994; 5:429–433.
9. Chen S, Wang D, Yuan C, Wang X, Zhang P, Gu X. Template synthesis of the polypyrrole tube and its bridging in vivo sciatic nerve regeneration. Journal of Materials Science Letters. 2000; 19:2157–2159.
10. Shi G, Rouabhia M, Wang Z, Dao L, Zhang Z. A novel electrically conductive and biodegradable composite made of polypyrrole nanoparticles and polylactide. Biomaterials. 2004; 25:2477–2488. [PubMed: 14751732]
11. Wong J, Langer R, Ingber D. Electrically conducting polymers can noninvasively control the shape and growth of mammalian cells. Proceedings of the National Academy of Sciences of the United States of America. 1994; 91:3201–3204. [PubMed: 8159724]
12. Schmidt C, Shastri V, Vacanti J, Langer R. Stimulation of neurite outgrowth using an electrically conducting polymer. Proceedings of the National Academy of Sciences of the United States of America. 1997; 94:8948–8953. [PubMed: 9256415]

13. Gilmore K, Kita M, Han Y, Gelmi A, Higgins M, Moulton S, Clark G, Kapsa R, Wallace G. Skeletal muscle cell proliferation and differentiation on polypyrrole substrates doped with extracellular matrix components. Biomaterials. 2009; 30:5292–5304. [PubMed: 19643473]
14. Guimard N, Sessler J, Schmidt C. Toward a biocompatible and biodegradable copolymer incorporating electroactive oligothiophene units. Macromolecules. 2009; 42:502–511. [PubMed: 20046223]
15. Lee J, Bashur C, Goldstein A, Schmidt C. Polypyrrole-coated electrospun PLGA nanofibers for neural tissue applications. Biomaterials. 2009; 30:4325–4335. [PubMed: 19501901]
16. Wan Y, Wu H, Wen D. Porous-conductive chitosan scaffolds for tissue engineering, 1-preparation and characterization. Macromolecular Bioscience. 2004; 4:882–890. [PubMed: 15468297]
17. Gogolewski, S. Desk Reference of Functional Polymers, Synthesis and Applications. Arshady, R., editor. Washington, DC: American Chemical Society; 1996. p. 657
18. Lelah, M.; Cooper, S. Polyurethanes in medicine. Boca Raton, FL: CRC Press; 1986.
19. Guan J, Fujimoto K, Sacks M, Wagner W. Preparation and characterization of highly porous, biodegradable polyurethane scaffolds for soft tissue applications. Biomaterials. 2005; 26:3961–3971. [PubMed: 15626443]
20. Mcdevitt T, Woodhouse K, Hauschka S, Murry C, Stayton P. Spatially organized layers of cardiomyocytes on biodegradable polyurethane films for myocardial repair. Journal of Biomedical Materials Research. 2003; 66A:586–595. [PubMed: 12918042]
21. Bonzani I, Adhikari R, Houshyar S, Mayadunne R, Gunatillake P, Stevens M. Synthesis of two-component injectable polyurethanes for bone tissue engineering. Biomaterials. 2007; 28:423–433. [PubMed: 16979756]
22. Carlberg B, Axell M, Nannmark U, Lieu J, Kuhn H. Electrospun polyurethane scaffolds for proliferation and neuronal differentiation of human embryonic stem cells. Biomedical Materials. 2009; 4:1–7.
23. Siepe M, Giraud M, Liljensten E, Nydegger U, Menasche P, Carrel T, Tevaearai H. Construction of skeletal myoblast-based polyurethane scaffolds for myocardial repair. Artificial Organs. 2007; 31:425–433. [PubMed: 17537054]
24. Keohan F, Wei X, Wongsarnpigoon A, Lazaro E, Darga J, Grill W. Fabrication and evaluation of conductive elastomer electrodes for neural stimulation. Journal of Biomaterials Science - Polymer Edition. 2007; 18:1057–1073. [PubMed: 17705998]
25. Robila G, Diaconu I, Buruiana T, Buruiana E, Coman P. Carboxylated polyurethane anionomers and their composites with polypyrrole. Journal of Applied Polymer Science. 2000; 75:1385–1392.
26. Deligoz H, Tieke B. Conducting composites of polyurethane resin and polypyrrole: solvent-free preparation, electrical, and mechanical properties. Macromolecular Materials and Engineering. 2006; 291:793–801.
27. Wang Z, Roberge C, Wan Y, Dao L, Guidoin R, Zhang Z. A biodegradable electrical bioconductor made of polypyrrole nanoparticle/poly(D,L -lactide) composite: A preliminary in vitro biostability study. Journal of Biomaterials Research Part A. 2003; 66A:738–746.
28. Uhlir AJ. The Bell System Technical Journal. 1955; 34:105.
29. Smits F. The Bell System Technical Journal. 1958; 37:711–718.
30. Choi J, Lee S, Christ G, Atala A, Yoo J. The influence of electrospun aligned poly(epsilon-caprolactone)/collagen nanofiber meshes on the formation of self-aligned skeletal muscle myotubes. Biomaterials. 2008; 29:2899–2906. [PubMed: 18400295]
31. Kang H, Geckeler K. Enhanced electrical conductivity of polypyrrole prepared by chemical oxidative polymerization: effect of the preparation technique and polymer additive. Polymer. 2000; 41:6931–6934.
32. Santerre J, Woodhouse KA, Laroche G, Labow R. Understanding the biodegradation of polyurethanes: From classical implants to tissue engineering materials. Biomaterials. 2005; 26:7457–7470. [PubMed: 16024077]
33. Kidane A, Burriesci G, Cornejo P, Dooley A, Sarkar S, Bonhoeffer P, Edirisinghe M, Seifalian A. Current developments and future prospects for heart valve replacement therapy. Journal of Biomedical Materials Research Part B: Applied Biomaterials. 2009; 88B:290–303.

34. Bi X, Pei Q. An electrically-conductive composite prepared by electrochemical polymerization of pyrrole into polyurethane. Synthetic Metals. 1987; 22:145–156.

35. Wang Y, Sotzing G, Weiss R. Preparation of conductive polypyrrole/polyurethane composite foams by in situ polymerization of pyrrole. Chemistry of Materials. 2008; 20:2574–2582.

36. Seal B, Ortero T, Panitch A. Polymeric biomaterials for tissue and organ regeneration. Materials Science & Engineering: R: Reports. 2001; 34:147–230.

37. Wang X, Gu X, Yuan C, Chen S, Zhang P, Zhang T, Yao J, Chen F, Chen G. Evaluation of biocompatibility of polypyrrole in vitro and in vivo. Journal of Biomedical Materials Research: Part A. 2004; 68:411–422. [PubMed: 14762920]

38. Miller D, Thapa A, Haberstroh K, Webster T. Endothelial and vascular smooth muscle cell function on poly(lactic-co-glycolic acid) with nano-structured surface features. Biomaterials. 2004; 25:53–61. [PubMed: 14580908]

39. Sanger J, Chowrashi P, Shaner N, Spalthoff S, Wang H, Freeman N, Sanger J. Myofibrillogenesis in skeletal muscle cells. Clinical Orthopaedics and Related Research. 2002; Suppl S:S153–S162. [PubMed: 12394464]

40. Ateh D, Navsaria H, Vadgama P. Polypyrrole-based conducting polymers and interactions with biological tissues. J R Soc Interface. 2006; 3:741–752. [PubMed: 17015302]

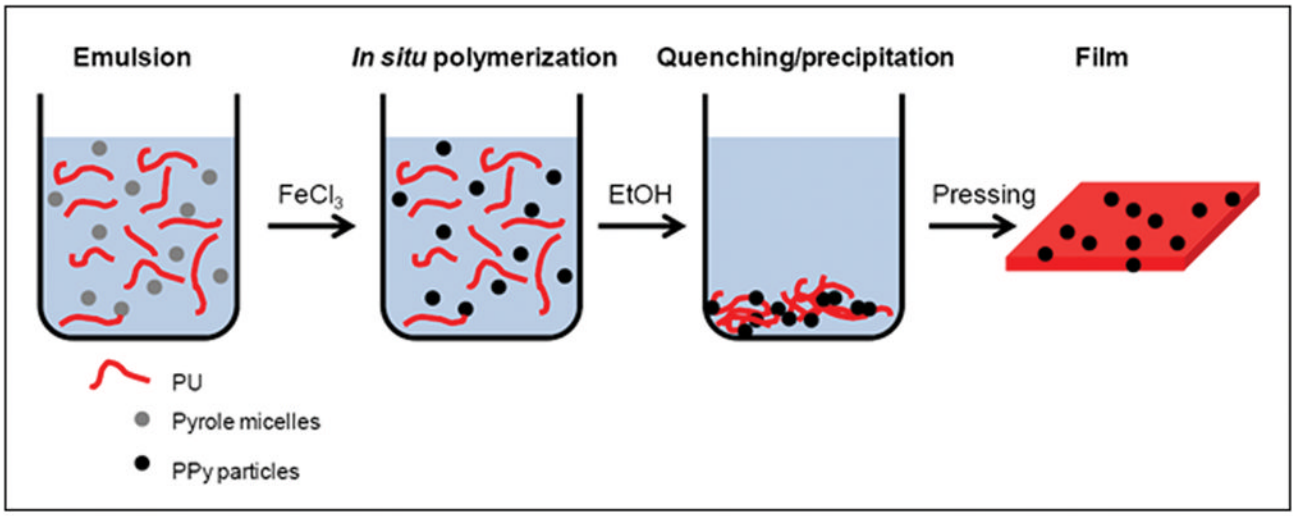

Figure 1.
Schematic of PPy-PU composite synthesis. Pyrrole was emulsified in PU/chloroform solution containing SDS with vigorous agitation. Then, by dropwise addition of $FeCl_3$, PPy nanoparticles were polymerized *in situ*. The reaction was quenched and the precipitant was washed with ethanol. Composite melt was molded into films.

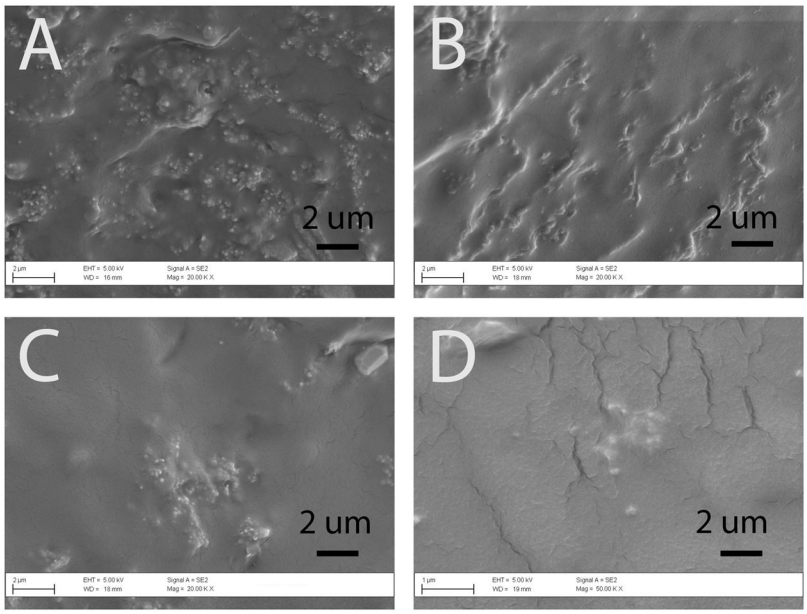

Figure 2.

Scanning electron micrographs of the surfaces of PPy-PU composites. (A) 1:100, (B) 1:20, (C) 1:10, and (D) 1:5 (Mag = ×20k) of PPy:PU. With increase in PPy portions in the composites, the numbers of PPy particles observed increased. PPy particles were interspersed within the PU housing of the composite.

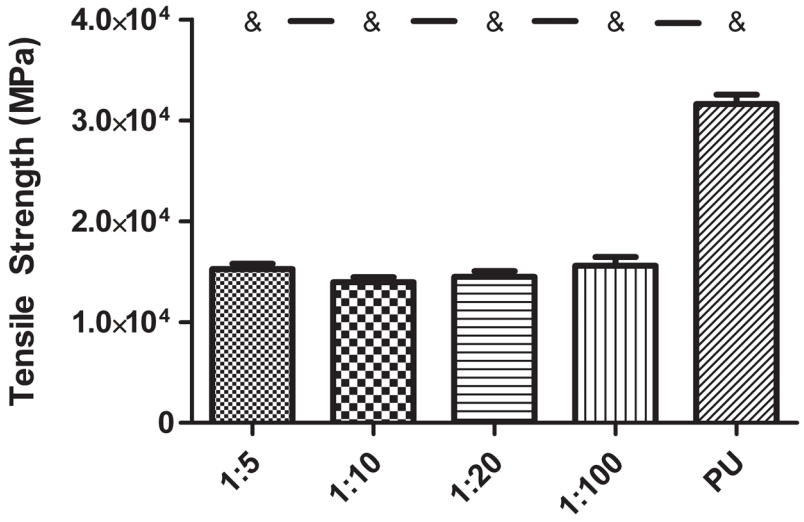

Figure 3.
Tensile strength of PPy- PU composites and PU. PPy-PU composites had an overall reduction in strength (MPa) with incorporation of increasing weight ratio of PPy:PU. '&' represents statistical significance when compared to the PU group. Error bars indicate standard deviation.

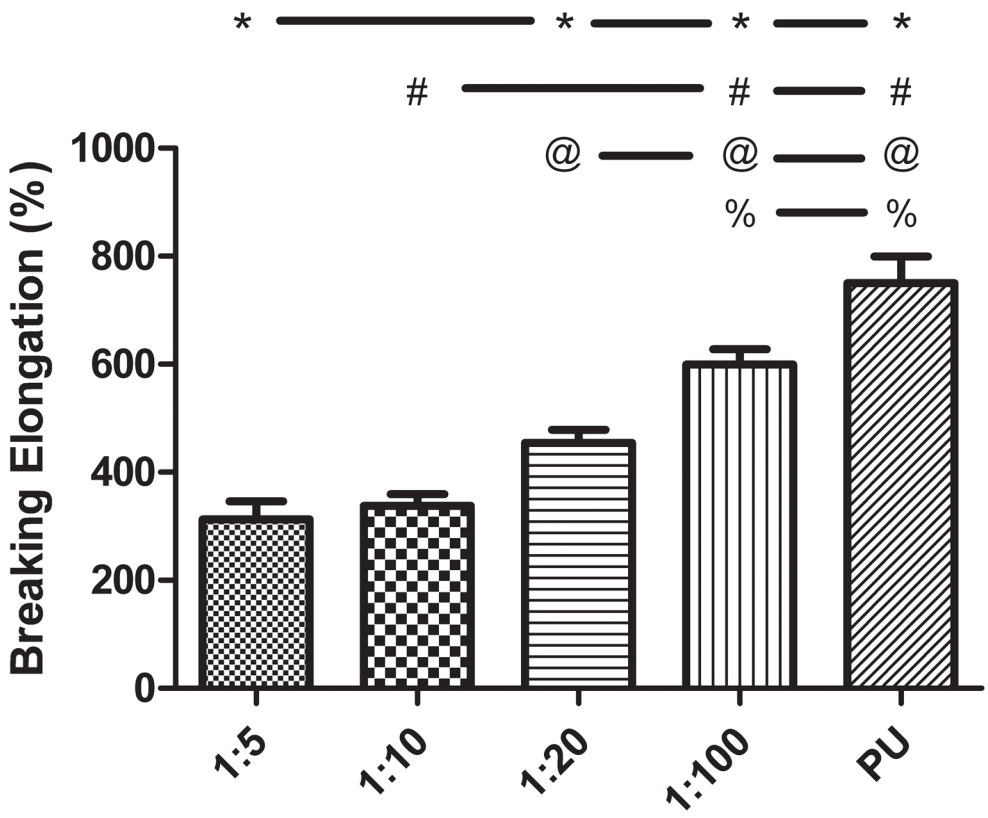

Figure 4.
Breaking elongation of PPy-PU composites and PU. PPy-PU composites demonstrated decreasing maximal stretching capacity (% of original length) as the weight ratio of PPy:PU was increased. '*', '#', '@', '%' represents statistical significance when compared to the 1:5, 1:10, 1:20, 1:100 of PPy:PU group, respectively. Error bars indicate standard deviation.

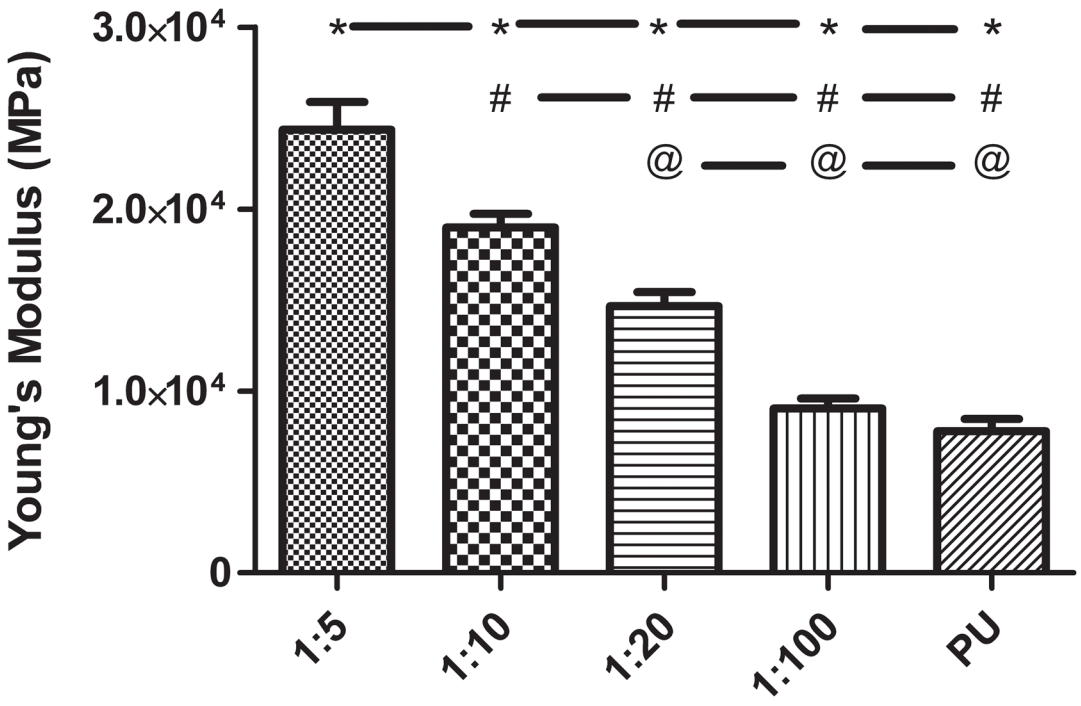

Figure 5.
Young's modulus of PPy-PU composites and PU. PPy-PU composites showed a trend of increasing material stiffness (MPa) as the weight ratio of PPy:PU was increased. '*', '#', '@' represents statistical significance when compared to the 1:5, 1:10, 1:20 of PPy:PU group, respectively. Error bars indicate standard deviation.

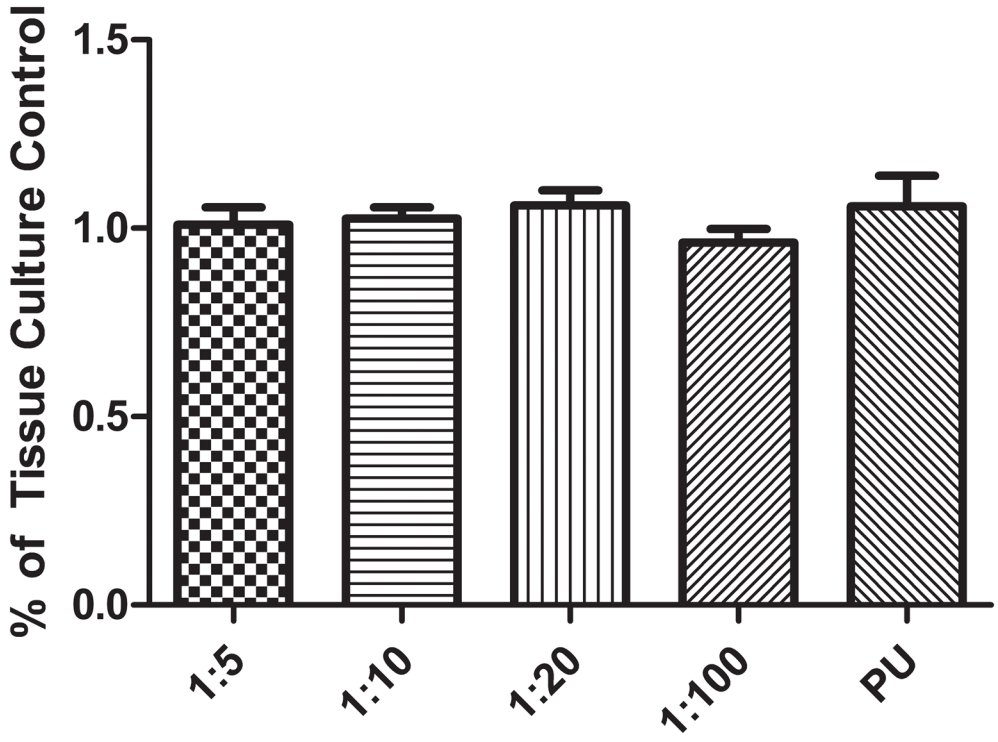

Figure 6.

Cytocompatibility of PPy-PU composites and PU. C2C12 myoblasts were seeded and cultured on tissue culture well plate for 24 hours in advance. The PU and PPy-PU composites were added to wells containing myoblasts. Following additional 48 hours of incubation with the materials, metabolic activities of the cells were meaured and normalized to the negative (tissue culture) control. Cellular metabolism was analyzed using MTS reagents and absorbance was measured at 470 nm (n=3). No experimental groups were statistically different. Error bars indicate standard deviation.

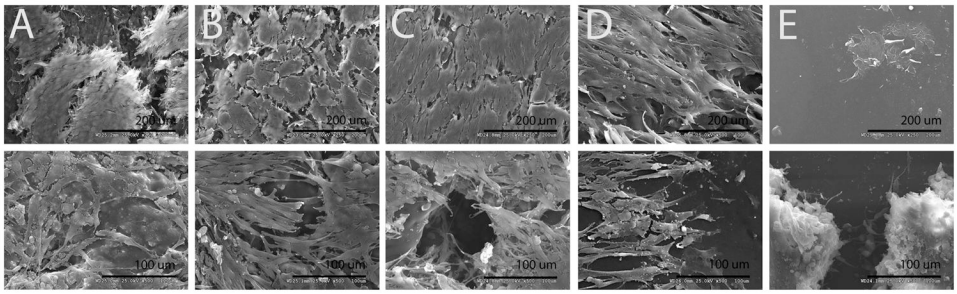

Figure 7.

Cell-scaffold interaction on PPy-PU composites and PU. Scanning electron micrographs of C2C12 myoblasts directly cultured on PU and PPy-PU composites for 24 h. (A) 1:5, (B) 1:10, (C) 1:20, (D) 1:100 of PPy:PU, and (E) PU. The lower magnificiation images (top, ×250) were seeded at an initial density of 2.5×10^5 cells per cm^2. The higher magnification images (bottom, ×500) were seeded at an initial density of 1.0×10^6 cells per cm^2. (A), (B), (C), (D) demonstrate diverse cell-material interactions while (E) shows cells 'caked on' the PU base.

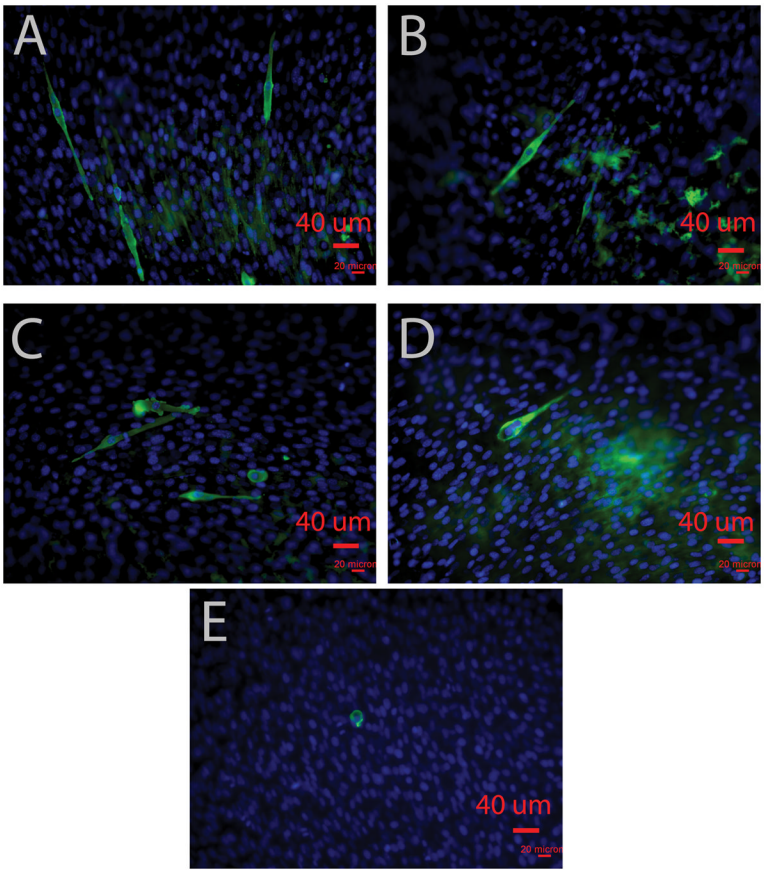

Figure 8.

Myotube differentiation of C2C12 myoblasts on PPy-PU composites and PU. Fluorescent images of C2C12 myoblasts on composite films (A) 1:5, (B) 1:10, (C) 1:20, (D) 1:100 of PPy:PU, and (E) PU. Myosin heavy chain (MHC) MF20 was stained in green, and DAPI was counterstained in blue. Images were taken by using a fluorescence microscope (×200).

Table 1

Conductivities of PPy-PU composites.

PPy:PU (mass ratio)	Average conductivity (± standard deviation) (S/cm)
1:5	$2.32\times10^{-6} \pm 2.97\times10^{-7}$
1:10 *	$2.00\times10^{-7} \pm 8.17\times10^{-8}$
1:20 *	$7.46\times10^{-10} \pm 1.88\times10^{-10}$
1:100 *	$9.95\times10^{-11} \pm 8.03\times10^{-11}$

* signifies statistical significance when compared to 1:5 of PPy:PU.